Coupled Plasmon-Waveguide Resonance Spectroscopy Studies of the Cytochrome b_6f/Plastocyanin System in Supported Lipid Bilayer Membranes

Z. Salamon,* D. Huang,# W. A. Cramer,# and G. Tollin*
*Department of Biochemistry, University of Arizona, Tucson, Arizona 85721, and #Department of Biological Sciences, Purdue University, W. Lafayette, Indiana 47907 USA

ABSTRACT The incorporation of cytochrome (cyt) b_6f into a solid-supported planar egg phosphatidylcholine (PC) bilayer membrane and complex formation with plastocyanin have been studied by a variant of surface plasmon resonance called coupled plasmon-waveguide resonance (CPWR) spectroscopy, developed in our laboratory. CPWR combines greatly enhanced sensitivity and spectral resolution with direct measurement of anisotropies in refractive index and optical extinction coefficient, and can therefore probe structural properties of lipid-protein and protein-protein interactions. Cyt b_6f incorporation into the membrane proceeds in two stages. The first occurs at low protein concentration and is characterized by an increase in total proteolipid mass without significant changes in the molecular order of the system, as demonstrated by shifts of the resonance position to larger incident angles without changing the refractive index anisotropy. The second stage, occurring at higher protein concentrations, results in a decrease in both the mass density and the molecular order of the system, evidenced by shifts of the resonance position to smaller incident angles and a large decrease in the membrane refractive index anisotropy. Plastocyanin can bind to such a proteolipid system in three different ways. First, the addition of plastocyanin before the second stage of b_6f incorporation begins results in complex formation between the two proteins with a K_D of ~10 μM and induces structural changes in the membrane that are similar to those occurring during the second stage of complex incorporation. The addition of larger amounts of plastocyanin under these conditions leads to nonspecific binding to the lipid phase with a K_D of ~180 μM. Finally, the addition of plastocyanin after the completion of the second phase of b_6f incorporation results in tighter binding between the two proteins ($K_D \approx 1$ μM). Quantitation of the binding stoichiometry indicates that two plastocyanin molecules bind tightly to the dimeric form of the cyt b_6f complex, assuming random insertion of the cytochrome into the bilayer. The structural basis for these results and formation of the proteolipid membrane are discussed.

INTRODUCTION

The interactions between membrane-associated proteins and lipids play an essential role in the functioning of a wide variety of cell membrane systems, including those in which cellular signals are mediated by lipid messengers that modulate protein functions (Culis and De Kruijf, 1979; Epand, 1991; Brown, 1994). Recent studies have shown that in other systems as well (e.g., rhodopsin; cf. Brown, 1994; Salamon et al., 1994, 1996), lipids can have a profound effect on the structure and function of integral membrane proteins, although the mechanisms of many of these interactions still have to be elucidated. Furthermore, it has become evident that the simple fluid-mosaic model of biological membranes (Singer and Nicolson, 1972), with its static view of a randomized lipid-protein composite, is inadequate to explain many of the complex properties of these systems (Mouritsen and Kinnunen, 1996). Many studies have shown (Brown, 1994; Salamon et al., 1994, 1996; Mouritsen and Kinnunen, 1996; Pinheiro et al., 1997; Jordi and Kruijff, 1995; Heimburg and Marsh, 1996; Salamon and Tollin, 1997) that protein-membrane interactions may have both thermodynamic and structural consequences, mediated by effects on the conformation of the protein as well as on the structure of the membrane, and that the structural organization of integral membrane proteins may control the functional state of the membrane. Thus studies of the organization and dynamics of lipid-protein assemblies are of considerable importance.

Elucidation of the microscopic properties of lipid and proteolipid assemblies represents a technically difficult challenge for several reasons: they are very thin structures comprising only one or two monolayers, they contain relatively small amounts of material located at the interface between two immiscible phases, and they are often both labile and structurally heterogeneous. As a result, only a limited number of studies have addressed the problem of lipid and protein structural organization in molecular films. In our laboratory, we have recently developed a variant of surface plasmon resonance (SPR) spectroscopy that can be applied to the structural and functional characterization of lipid and lipoprotein membranes (Salamon et al., 1997a). This involves a coupling of plasmon resonances in a thin metal film and waveguide modes in a dielectric overcoating (the technique is termed coupled plasmon-waveguide resonance (CPWR) spectroscopy) and combines a greatly enhanced sensitivity and spectral resolution with the ability to

Received for publication 18 February 1998 and in final form 22 June 1998.
Address reprint requests to Dr. Gordon Tollin, Department of Biochemistry, University of Arizona, Tucson, AZ 85721. Tel.: 520-621-3447; Fax: 520-621-9288; E-mail: gtollin@u.arizona.edu.

0006-3495/98/10/1874/12 $2.00

directly measure anisotropies in refractive index and optical absorption coefficient in a proteolipid membrane adsorbed to the surface of the overcoating (Salamon et al., 1997a). In the present experiments, we have utilized self-assembled, solid-supported planar lipid bilayer membranes and CPWR spectroscopy to investigate the mechanism and structural consequences of the incorporation of the cytochrome (cyt) b_6f complex into a lipid membrane, and to directly measure the binding parameters of the interaction between plastocyanin and such a cyt b_6f-containing lipid bilayer.

The cyt b_6f complex is one of three integral membrane protein complexes involved in electron transport in oxygenic photosynthesis. The complex accepts electrons from the oxygen-producing photosystem II reaction center, donates electrons to the $NADP^+$-reducing photosystem I reaction center, and contributes to the electrochemical proton gradient that drives ATP synthesis (Cramer et al., 1991). It is homologous in many aspects to the cyt bc_1 complex of the respiratory chains of the mitochondrion and photosynthetic bacteria. The b_6f complex comprises four subunits with a molecular mass greater than 18 kDa. Three of them, cyt b_6, cyt *f*, and Rieske iron-sulfur protein, contain redox prosthetic groups. The fourth subunit is involved together with cyt b_6 and Rieske protein in forming the oxidizing plastoquinol binding site (Cramer et al., 1996). The complex also contains at least three additional small hydrophobic polypeptides (~4 kDa). The total molecular mass of the seven-subunit monomeric complex is 110 kDa (Breyton et al., 1994). The redox partners of cyt *f* are its donor, the Rieske protein, and its acceptor, the soluble copper protein plastocyanin, which carries electrons to the photosystem I reaction center.

The b_6f complex has the unusual property that the subunits can be separated from the complex and from each other at alkaline pH (Szczepaniak et al., 1991; Cramer et al., 1994b). This implies that, unlike in many other membrane proteins (Cramer et al., 1994b), the attractive forces arising from intramembrane hydrophobic, hydrogen bonding, and van der Waals interactions between the subunits are relatively weak. As a consequence, the electrostatic repulsive force exerted between the subunits at alkaline pH, arising from the net excess negative charge on the peripheral polypeptide segments, is sufficient to cause the subunits of the complex to separate in the membrane. In addition, it is known that the b_6f complex, isolated predominantly in the dimeric form, can dissociate to a monomeric, relatively inactive form (Szczepaniak et al., 1991) from which the Rieske protein may be missing (Bald et al., 1992). The relatively weak intramembrane forces between subunits apparently facilitate interconversion of monomer and dimer forms of the complex (Cramer et al., 1994b).

Plastocyanin is a small copper-containing protein (10.5 kDa) that is also a part of the electron transfer chain in photosynthetic cyanobacteria, algae, and higher plants (for reviews see Gross et al., 1993; Pearson et al., 1996; Sigfridsson et al., 1997). The three-dimensional structure of poplar plastocyanin has been determined at 1.3 Å resolution (Guss et al., 1992) and shows that the protein consists of a single polypeptide chain of 99 residues, forming an eight-stranded β-barrel. As noted above, the functional role of plastocyanin is to carry electrons from cyt *f* to the reaction center chlorophyll dimer, P700, in photosystem I. The specific mechanism of interaction between plastocyanin and cyt *f* in the chloroplast, which involves complex formation and electron transfer, has not been completely elucidated (Pearson et al., 1996; Soriano et al., 1996). The most probable hypothesis for in vitro interprotein electron transfer (Pearson et al., 1996; Soriano et al., 1996) assumes that the interaction is mediated by electrostatic attraction between the prominent basic region of cyt *f* located at the interface of its large and small domains and an acidic patch on the surface of plastocyanin. There is, however, experimental evidence which indicates that the reduction of the plastocyanin copper center can also occur at comparable rates via docking to a hydrophobic surface patch (Qin and Kostic, 1993). A role for a hydrophobic interaction was also proposed from the biphasic response to ionic strength of the in vitro rate of the turnip cyt *f*–plastocyanin reaction (Meyer et al., 1993) and from interaction of plastocyanin with supported lipid bilayer membranes (Salamon and Tollin, 1992). All of these factors have recently been combined into a mechanism for the in vitro reaction in which initial electrostatic guidance and contact between the two proteins is followed by nonpolar interactions that mediate movement of plastocyanin on the surface of cyt *f*, allowing the copper to come closer to the heme (Pearson et al., 1996; Martinez et al., 1994).

As will be demonstrated below, the results of the present CPWR experiments clearly reveal that incorporation of cyt b_6f complex into a self-assembled solid-supported lipid membrane is a complex, protein concentration-dependent process involving two stages, the second of which results in large structural and compositional changes in the lipid membrane. Furthermore, the presence of plastocyanin influences these processes by binding to the cyt b_6f complex with a much higher affinity after the second stage of incorporation has occurred.

MATERIALS AND METHODS

Purification of cyt b_6f complex and plastocyanin

Cytochrome b_6f complex was purified from spinach chloroplasts as described in Huang et al. (1994), and by a generally similar procedure from the thermophilic cyanobacterium *Mastigocladus laminosus* (Huang et al., manuscript in preparation), and resuspended in 30 mM Tris-HCl, pH 7.8, containing 50 mM NaCl, 1 mM $MgCl_2$, and 30 mM β-octylglucoside. The purified complex from chloroplasts and *Mastigocladus laminosus*, respectively, was characterized by typical turnover activities of ~100 (25°C) and ~450 (35°C) electrons transferred to cyt *f* per second from decyl-plastoquinol. Plastocyanin was obtained from spinach by the procedure of Yocum (1982) and was characterized spectrophotometrically.

Preparation of egg PC bilayer membranes

Lipid bilayer membranes were formed on a silica surface deposited on a silver film (Salamon et al., 1997a) from a solution containing either 10

mg/ml egg PC in squalene (Fluka)/butanol (either 1% or 1.5%; v/v) or 6 mg/ml egg PC in squalene/butanol (1%; v/v), using a procedure originally developed to form freely suspended lipid bilayer membranes separating two aqueous solutions (Mueller et al., 1962). The method, which is based on the interaction between the hydrophilic silica surface and amphipathic lipid molecules, involves spreading a small amount of lipid bilayer-forming solution via a Hamilton microsyringe across an orifice in a Teflon sheet that separates the silica film from the aqueous phase (Salamon et al., 1997a). The surface of the silica, covered with a thin layer of water (Gee et al., 1990; Silberzan et al., 1991), attracts the polar groups of the lipid molecules, thus forming an adsorbed lipid monolayer with the hydrocarbon chains oriented toward the bulk lipid phase. Subsequent to this first step of lipid membrane formation, the main body of the sample cell (Salamon et al., 1997a) is filled with a buffer solution (10 mM Tris-HCl, 5 mM KCl; pH 7.5). This initiates the second step, which involves a thinning process, i.e., formation of both the second monolayer and a Plateau-Gibbs border that anchors the bilayer membrane to the Teflon spacer, allowing the excess of lipid and solvent to move out of the Teflon orifice.

Preparation of PC bilayer membranes containing cyt b_6f complex and plastocyanin binding

Cyt b_6f complex was incorporated into a preformed lipid membrane deposited on the surface of the silica film by adding small aliquots of a concentrated solution (~115 μM) of either thermophilic cyanobacterial (*Mastigocladus laminosus*) or spinach cyt b_6f complex, in 30 mM Tris-HCl, pH 7.8, containing 50 mM NaCl, 1 mM $MgCl_2$, and 30 mM octyl glucoside, to the aqueous compartment of the CPWR cell. The latter contained ~2 ml of 10 mM Tris-HCl buffer with 5 mM KCl at pH 7.5; addition of the protein solution thereby diluted the detergent to a final concentration in the range of 0.3–3.0 mM, significantly below its critical micelle concentration (cmc = 25 mM), allowing transfer of cyt b_6f into the supported egg PC bilayer. After the CPWR spectral changes produced upon the addition of each aliquot of protein reached saturation (~20 min), the resonance spectra were recorded. Identical results were obtained with either of the two cyt b_6f complexes. To determine if denaturation of the b_6f complex occurred upon dilution of the detergent to below the cmc, we have carried out parallel experiments with the spinach protein under these same conditions, measuring reduced minus oxidized difference spectra (data not shown). Only relatively small spectral changes occurred over a 20-min time period (the cyt *b*:cyt *f* heme ratio went from 1.8:1 to 1.62:1), indicating that the protein was not extensively denatured by dilution. To measure plastocyanin binding, small aliquots of concentrated solutions of plastocyanin (~1 mM) in Tris buffer were added to the aqueous compartment of the CPWR cell within ~1 min after the end of each of the two stages of cyt b_6f complex incorporation (see below).

Coupled plasmon-waveguide resonance spectroscopy

The CPWR apparatus and the experimental and theoretical data analysis procedures are the same as those used with conventional surface plasmon resonance (SPR) spectroscopy (Salamon et al., 1997b,c; Salamon and Tollin, 1998). Those aspects of the methodology that are unique to the CPWR application have recently been described elsewhere (Salamon et al., 1997a). Here we present only a brief summary of the technology. The method involves a coupling of plasmon resonances in a thin metal film and waveguide modes in a dielectric overcoating, and thus combines characteristic features of both waveguide spectroscopy (high sensitivity and spectral resolution and the ability to direcly measure anisotropies in refractive index and optical absorption coefficient in a sensing layer) and SPR spectroscopy (simple and convenient optical coupling arrangements and a complete isolation of the optical probe from the system under investigation). Spectroscopic measurements with CPWR devices are based on the resonant excitation of electromagnetic modes of the structure by both TM (transverse magnetic; *p*) and TE (tranverse electric; *s*) polarized components of cw (continuous wave) laser light (He-Ne with either λ = 632.8 nm [red light], or λ = 543.5 nm [green light] were used) within the available incident angles under total internal reflection conditions, as previously described (Salamon et al., 1997a). As a consequence, anisotropies in both refractive index and optical absorption coefficient can be determined with high precision and sensitivity.

According to electromagnetic theory, the optical properties of thin-film materials (including lipid-protein systems) are characterized by their thickness (*t*) and by a complex dielectric constant, which includes the refractive index (*n*) and the extinction coefficient (*k*) (Salamon et al., 1997a, b, c; Salamon and Tollin, 1998). The CPWR phenomenon is a straightforward consequence of the application of thin-film electromagnetic theory. The influence of film optical parameters (*n*, *k*, and *t*) on the characteristics of the CPWR spectrum is completely contained in this theory. For any dielectric layer, including lipid and proteolipid membranes, the number of measured CPWR curve parameters (i.e., position, width, and depth of the resonance curve) equals the number of unknown optical parameters, and thus the latter can be readily evaluated. Because these are well separated in the equations, they can be uniquely evaluated from the spectra, using a nonlinear least-squares technique to fit a theoretical resonance curve to an experimental one. In addition, because the refractive index (*n*) directly reflects a mass density (defined as mass per unit volume of deposited material), one can obtain the total deposited mass from the *t* and *n* parameters (Salamon et al., 1997a-c; Salamon and Tollin, 1998). If *t* is constant, an increase in the resonance angle can be associated with an increase in mass density within the film, and vice versa. As will be seen below, this is quite important in the context of the present experiments. Furthermore, these three optical parameters (*t, n, k*) can be evaluated for both polarizations, thereby producing enough experimental data to characterize the following structural parameters of the thin films: thickness, orientation of molecules (by measuring the anisotropy in *n*), and the orientation of chromophores attached to the molecules within the sensing layer (by measuring the anisotropy of *k*). In the experiments descibed in this work, the light wavelengths used (see above) are located away from the absorption maxima of the cyt b_6f chromophore centers, and thus the extinction coefficient (*k*) represents mainly scattered light due to imperfections in the proteolipid membrane structure.

In the present experiments, the CPWR interface designs were manufactured by Denton Vacuum (Moorestown, NJ). They contained two optically active layers of different thicknesses, silver and SiO_2, deposited on a glass prism. Special care has been taken in the manufacture to produce durable, long-lasting films, which can be ultrasonically cleaned and reused for many measurements.

RESULTS

Biphasic cyt b_6f incorporation

The incorporation of cyt b_6f into a solid-supported planar egg PC bilayer was followed by monitoring steady-state CPWR spectra obtained after the addition of a small aliquot of a concentrated solution of protein, dissolved in an octyl glucoside-containing buffer, to the aqueous compartment of a CPWR cell. As we have previously demonstrated with other integral membrane proteins (Salamon et al., 1994, 1996; Salamon and Tollin, 1996a, b), typical spectral changes resulting from protein incorporation into the bilayer upon dilution of the detergent to below its cmc involve both a shift of the resonance position to larger incident angles and alterations in the resonance curve shape due to changes in the resonance depth and width. In the case of cyt b_6f complex incorporation, this typical paradigm was significantly modified in that a dramatically different pattern of spectral changes was obtained at low and high protein

concentrations within the CPWR cell. At low concentrations of the protein (up to 4.2 μM; see Fig. 1 *A, curve 2*) there was a shift of the resonance position to a larger angle of incidence, accompanied by an increase in the depth and a decrease in the width of the resonance curve as compared to that obtained with the lipid bilayer membrane before b_6f addition (*curve 1*). This corresponds to the usual pattern of spectral changes that we have observed previously with other membrane proteins, resulting from an increase in mass within the bilayer region due to protein insertion. However, at higher b_6f concentrations (6.3 μM and 8.4 μM; Fig. 1 *A, curves 3 and 4*) this pattern was replaced by a reverse shift of the resonance position, with even larger changes in the shape of the resonance curve. A similar pattern was observed with *s*-polarization (data not shown). The reversal of the shift direction at higher protein concentrations and the changes in spectral shape are clearly illustrated by the data in Fig. 1 *A*. Although we have not accurately measured the time dependence of either the first or second phases, they occur in a similar time range, with each addition of protein equilibrating within 15–25 min. It has to be emphasized that addition of the same amounts of detergent solution without protein to the aqueous compartment of the CPWR cell does not measurably change the resonance spectra.

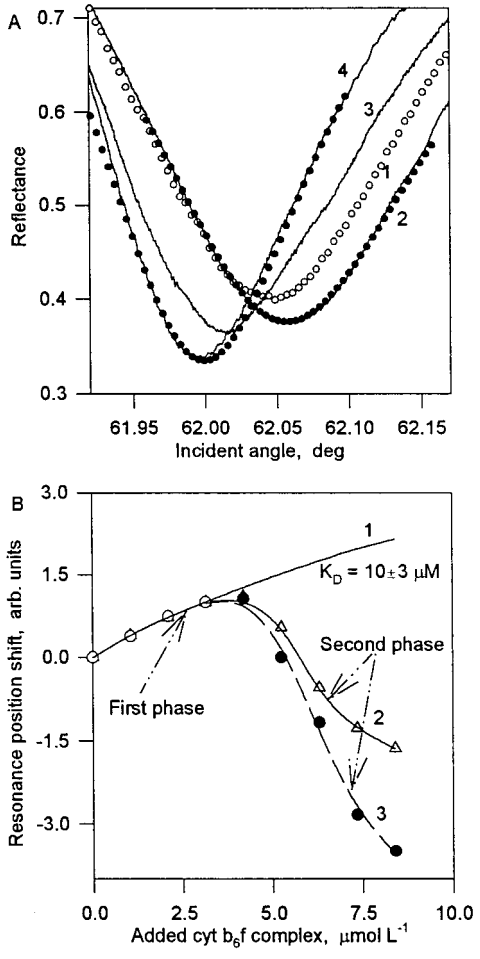

FIGURE 1 (*A*) Typical CPWR spectra obtained with a lipid membrane formed from a solution of 10 mg/ml egg PC in butanol containing 1.5% squalene and *p*-polarized 632.8 nm laser light. Curve 1 (*open circles*) was obtained without cyt b_6f, whereas curves 2–4 were obtained after the addition of different amounts of protein to the sample compartment of the CPWR cell. Curve 2 corresponds to the end of the first phase (taken at 4.2 μM cyt b_6f complex in the buffer compartment of the sample cell), and curves 3 (at 6.3 μM cyt b_6f) and 4 (at 8.4 μM cyt b_6f) to the end of the second phase of protein incorporation (see text). Closed circles in spectra 2 and 4 represent theoretical fits to the data (see text for discussion). (*B*) Dependence of the resonance minimum position on the cyt b_6f complex concentration in the aqueous phase during protein incorporation into a PC bilayer membrane (as described in *A*) containing varying amounts of squalene: 1% (v/v): ▲, first phase of incorporation; △, second phase; 1.5% (v/v): ○, first phase; ●, second phase. Curves show nonlinear least-squares fits to either hyperbolic (curve 1; K_D = 10 μM) or sigmoidal (curves 2 and 3) functions.

The process of cyt b_6f incorporation was also shown to be dependent on the lipid membrane composition and structure, which in the present experiments have been changed by varying the amount of squalene used in forming the bilayer. Fig. 1 *B* shows the *p*-polarized resonance position shifts as a function of b_6f concentration for two lipid bilayer membranes, containing either 1.5% (*circles*) or 1% (*triangles*) squalene (v/v) in a butanol solution of 10 mg/ml egg PC. The structural properties of these two lipid membranes are quite different, as indicated by the optical parameters presented in Table 1, which were obtained by fitting the experimental CPWR curves by the procedures described previously (Salamon et al., 1996, 1997a-c). This is due to changes in the packing of fatty acid tails in the membrane interior caused by the incorporation of different amounts of squalene, which results in increases in both the bilayer thickness and its optical anisotropy (for further details see the discussion of Table 2 below) (Salamon et al., 1996). For ease of comparison, the individual data points in Fig. 1 *B* have been normalized to the maximum shift to larger angles that occurred during the experiment. The lines represent, for both membranes, theoretical hyperbolic fits (*curve 1*) or sigmoidal fits (*curves 2 and 3*) to the experimental data. It can clearly be seen from these data that the second phase of the incorporation is more significantly influenced by the properties of the lipid membrane than is the first phase. It is also important to note that the first phase can be fit by a simple hyperbolic function (with an apparent $K_D = 10 \pm 3$ μM), whereas the second phase is evidently sigmoidal, indicating that different molecular processes are responsible for the measured spectral changes in the two concentration ranges. These results, together with the fact that during the second phase the resonance position shifts in the direction opposite that which should occur in the case of a simple increase in the mass of incorporated cyt b_6f, strongly indicate that the spectral alterations in the second phase are generated by structural changes within the proteolipid membrane involving a decrease in mass density (see above). In other words, the usual spectral changes due to insertion of additional protein mass into the lipid membrane, which takes place during both phases, must be overridden in the second phase by even stronger effects due to structural

TABLE 1 Summary of the optical parameters obtained for lipid bilayers containing either 1% (1) or 1.5% (2) squalene, with or without cyt b_6f and with either *p*- or *s*-polarized 632.8-nm laser light*

			1			2		
			n	t (nm)	k	n	t (nm)	k
BLM; no b_6f		p	1.548	5.3	0.020	1.592	5.9	0.070
		s	1.480	5.2	0.030	1.505	5.9	0.052
BLM + b_6f (first phase)[#]	Protein-lipid layer	p	1.548	5.3	0.025	1.592	5.9	0.070
		s	1.480	5.2	0.030	1.505	5.9	0.052
	Protein-buffer layer	p	1.346	5.2	0.005	1.346	5.1	0
		s	1.348	5.2	0	1.340	5.0	0
BLM + b_6f (second phase)[§]	Protein-lipid layer	p	1.503	5.3	0.010	1.490	5.9	0.220
		s	1.465	5.2	0.010	1.440	5.9	0.012
	Protein-buffer layer	p	1.356	5.2	0	1.357	5.1	0
		s	1.361	5.2	0	1.358	5.0	0

n, Refractive index; t, thickness; k, extinction coefficient.
*The optical parameters have been obtained with the following accuracies: the refractive index ±0.001, the thickness ±0.1 nm, and the extinction coefficient ±0.002.
[#]Data taken at 4.2 μM cyt b_6f.
[§]Data taken at 8.4 μM cyt b_6f.

changes of the membrane that result from alterations in mass distribution. This will be discussed further below.

Characterization of the two phases of cyt b_6f incorporation

To quantitatively characterize these complex spectral changes we have used the following model. In the first stage of incorporation (data obtained at low protein concentrations in Fig. 1), a simple insertion of cyt b_6f into the lipid bilayer occurs, as has been observed with other transmembrane proteins integrating into solid-supported planar lipid membranes (Salamon et al., 1994, 1996, 1997b,c; Salamon and Tollin, 1996a,b, 1998). This can be described by a hyperbolic binding curve and produces a proteolipid structure consisting of two regions (see Fig. 2) in which the hydrophobic (integral) components of the b_6f complex are located within the bilayer interior forming a protein-lipid layer, and the hydrophilic (peripheral) portion of the protein extends outside the lipid membrane and forms an extramembrane protein-buffer layer. A more detailed description of such a two-layered model has previously been presented elswhere (Salamon et al., 1997c). For a membrane-spanning protein, there will be a protein-buffer layer on each side of the bilayer membrane. This becomes especially important when the protein is asymmetrical in shape and randomly inserts into the membrane, thereby producing two protein-buffer layers similar in both composition and optical properties, separated by the thickness of the lipid membrane (i.e., ~5.5 nm; note that this corresponds to an average thickness of the membrane, which includes the hydrated lipid headgroups; Salamon et al., 1996) and 1–2 nm of water formed by condensation of liquid on the flat SiO_2 surface (Gee et al., 1990; Silberzan et al., 1991). These two protein-buffer layers are essentially identical if the protein inserts randomly and can therefore be assumed to be a single layer in the modeling process used to obtain theoretical CPWR resonance curves (note that only a single protein-buffer layer is shown in Fig. 2). Such a model has been employed in this work; its justification is that it yields good fits to the data and reasonable dimensions for the protein molecules in the membrane, as will be described below.

It is also important to point out that insertion of the hydrophobic portion of a transmembrane protein into the lipid membrane interior results in the displacement of lipid molecules by protein (in the present membrane system, this

TABLE 2 Calculated values of the average refractive index (n_{av})[a], the refractive index anisotropy (A_n)[b], and the total mass (m_t) from the optical parameters of the bilayers given in Table 1

		1				2			
				m_t (μmol m^{-2})				m_t (μmol m^{-2})	
		n_{av}	A_n	Lipid	Protein	n_{av}	A_n	Lipid	Protein
BLM; no b_6f		1.503	0.048	7.4 ± 0.7	0	1.535	0.062	8.7 ± 0.9	0
BLM + b_6f (first phase)	Protein-lipid layer	1.503	0.048	7.2 ± 0.7	0.007 ± 0.001	1.535	0.062	8.5 ± 0.9	0.005 ± 0.001
	Protein-buffer layer	1.347	0			1.342	0.004		
BLM + b_6f (second phase)	Protein-lipid layer	1.478	0.026	4.0 ± 0.5	0.011 ± 0.003	1.458	0.036	4.0 ± 0.5	0.011 ± 0.003
	Protein-buffer layer	1.358	0.003			1.357	0		

[a]The estimated accuracy is ±0.001. [b]The error is ±0.002.

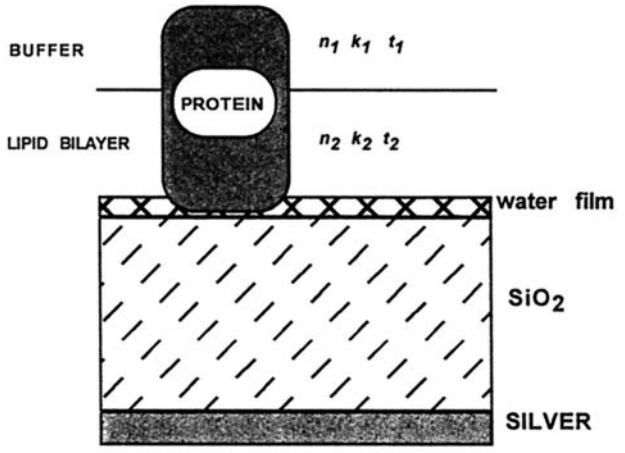

FIGURE 2 Schematic of the two-layer model (lipid-protein and buffer-protein) used for fitting CPWR data. Also shown are silver film and deposited hydrated SiO_2 layer. Water of hydration is included in the optical parameters of both layers.

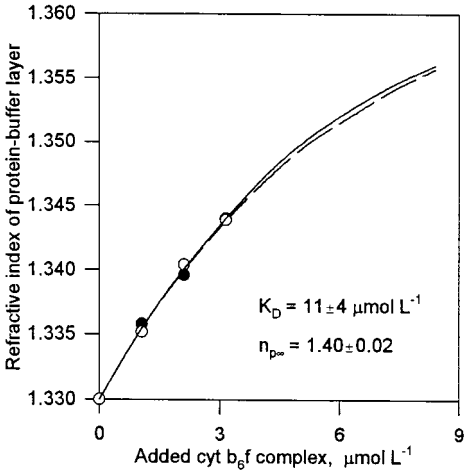

FIGURE 3 Refractive index of the protein-buffer layer of the two-layer proteolipid membrane model (see text) as a function of the cyt b_6f complex concentration in the aqueous phase, during the first phase of protein incorporation, obtained with a PC bilayer as described in Fig. 1 and containing either 1% (○, – – –) or 1.5% (●, ——) squalene, and *p*-polarized laser light. Solid and dashed lines represent nonlinear least-squares fits to a hyperbolic function; these yield the refractive indices of the protein-buffer layer for the second phase of protein incorporation and the apparent incorporation constant (K_D) and final value of the refractive index ($n_{p\infty}$).

excess lipid goes into the Plateau-Gibbs border, which anchors the membrane to the Teflon support). This process does not produce a significant change in the CPWR spectrum, because the refractive indices of lipid and protein are very similar (~1.5). Thus, during a simple insertion process of integral protein molecules whose dimensions are larger than the lipid membrane, the major portion of the resonance shift toward larger incident angles comes from the protein-buffer layer (the refractive indices of protein and buffer are quite different). In contrast to this, as we have noted above, the structural changes responsible for the observed reversal in the direction of the spectral shifts, which characterizes the second phase of protein incorporation, occur only in the protein-lipid layer. As we will demonstrate below, these latter changes are due to modifications in the ordering of the lipid and protein molecules in the bilayer membrane.

Using this framework, one can fit the experimental resonance curves with theoretical curves (for details see Salamon et al., 1997b,c) and thereby obtain the optical parameters of the proteolipid membrane during both phases of protein incorporation. Examples of such theoretical fits are given in Fig. 1 *A*. Fig. 3 shows the refractive index values for the protein-buffer layer obtained from fitting the experimental *p*-polarized resonance curves during the first phase of cyt b_6f incorporation into a lipid membrane containing either 1% (*closed circles*) or 1.5% (*open circles*) of squalene. Note that little or no difference exists between the two membranes. The solid lines correspond to hyperbolic fits to these experimental data points, yielding a K_D value of 11 ± 4 μM (note that this is in good agreement with the hyperbolic fit in Fig. 1 *B*). Extrapolation of the hyperbolic fit to infinite concentration of the b_6f complex results in a value for $n_{p\infty}$ that allows a calculation of the surface mass (packing) density (defined as mass per unit surface area) of the incorporated protein. The $n_{p\infty}$ value obtained in this way (1.40 ± 0.02) is somewhat low for close packing of an incorporated protein (a more typical value lies between 1.45 and 1.50; cf. Salamon et al., 1997b,c; Salamon and Tollin, 1998). This indicates that there is significant dilution of the protein within the bilayer, i.e., appreciable buffer is present in the protein-buffer layer (see Fig. 2; for further discussion see below).

To calculate the mass of cyt b_6f incorporated into the bilayer during the second phase, we have used the extrapolated *n* values obtained from the extensions of the curves in Fig. 3. This assumes that protein insertion precedes the structural changes that result in the observed negative shifts in resonance angle (i.e., that if these structural changes had not occurred, the *n* values would have increased along these hyperbolic curves). This allows us to calculate the optical parameters of the protein-lipid layer during the second phase of incorporation by theoretically fitting the latter resonance curves. The same assumptions and fitting procedures can be used with the *s*-polarized resonance data, which then generate a second set of optical parameters describing both phases of protein incorporation. Table 1 presents the values of refractive indices (*n*) and thicknesses (*t*) for both protein-lipid and protein-buffer layers obtained with both types of lipid membranes and both polarizations (optical extinction coefficient, *k*, values are also given, but the significance of these is less clear, inasmuch as they correspond mainly to light scattering effects; these will not be discussed further). The results show that the calculated total thickness of the cyt b_6f complex lies in the range of 10.4–11.0 nm for the two lipid membranes used here (corresponding to the sum of values for both protein-lipid and protein-buffer layers, as shown in Fig. 2). The same range of

values for the complex thickness has been independently obtained using both red (632.8 nm) and green (543.5 nm) laser wavelengths (data for latter not shown).

Although a projection map of the cyt b_6f complex has recently been determined at 8-Å resolution (Mosser et al., 1997), and therefore the diameters of both monomeric and dimeric molecules have been measured, there is still no high-resolution three-dimensional structure for the protein. The available spectroscopic, biochemical, genetic, and electron microscopy studies (Cramer et al., 1996; Mosser et al., 1997) have yielded only limited information about three-dimensional structure. Based on these investigations, estimated values for the length of the molecule vary from 8.3 nm for the complex from *Synechocystis* PCC 6803 to 11.0 nm for spinach cyt b_6f (Boekema et al., 1994). Thus we consider the thickness values presented in Table 1 as being in satisfactory agreement with the other estimates in the literature. The results in Table 1 also demonstrate that the protein-buffer layer shows only a minimal difference between the refractive indices measured with either *p*- or *s*-polarizations (i.e., a low refractive index anisotropy), indicating a very small degree of molecular order in this extramembrane region of the system.

The data in Fig. 3 and Table 1 and the Lorentz-Lorenz equation as previously described (Salamon et al., 1994, 1996; Salamon and Tollin 1996a,b) allow a calculation of the mass of protein inserted into the lipid bilayer membrane, using a molecular mass of 110 kDa for the cyt b_6f complex and assuming that the mass of the complex is equally divided between the two layers (see Fig. 2). Furthermore, the refractive indices obtained with *p*- and *s*-polarized light provide information on the molecular order of the system. As has previously been described (Salamon et al., 1997a), in the *p*-polarization case the electric vector is completely normal to the surface of the lipid membrane, whereas in *s*-polarization the electric vector is parallel to the surface of the lipid film. The anisotropy of the refractive index (A_n) can be defined as

$$A_n = (n_p^2 - n_s^2)/(n_{av}^2 + 2) \quad (1)$$

where n_{av} is an average value of the refractive index [$n_{av}^2 = 1/3(n_p^2 + 2n_s^2)$], and n_p and n_s are the refractive indices measured in the parallel and perpendicular directions within the lipid membrane. A_n can be related to the components of the mean polarizabilities along these two directions and to the anisotropy of the molecular shape (Den Engelson, 1976). In the present system, the anisotropy of the refractive indices and therefore the mean polarizabilities along the *p*- and *s*-polarization vectors are the direct result of orientation of the elongated molecules comprising the proteolipid membrane (Salamon et al., 1997a). Thus A_n is proportional to the degree of molecular order (S) (Pelzl, 1994), which is defined as follows:

$$S = 1/2(3\cos^2\theta - 1) \quad (2)$$

where θ is the tilt angle of the molecule to the surface normal. One can then calculate A_n from the measured n values and therefore evaluate changes in the molecular order of the proteolipid membrane that occur during the incorporation process.

Table 2 shows the results of calculations of the A_n values for the two stages of cyt b_6f incorporation, along with the total mass of lipid and protein, for the two types of lipid bilayer membranes used in these experiments. These results demonstrate several important facts regarding the properties of the proteolipid membrane:

(1) The optical parameters of the lipid bilayer (in particular n and t) are significantly changed by variation in the squalene content. This is in agreement with our previous measurements (Salamon et al., 1996), as well as with other studies of the role of incorporated hydrocarbons in lipid bilayer membranes using ellipsometry and x-ray reflectivity (Thoma et al., 1996). Such measurements indicate that increasing the amount of hydrocarbon solvent in the bilayer-forming solution causes an increase of both the bilayer thickness and its optical anisotropy. These effects involve hydrocarbon chain penetration into the hydrophobic interior of the lipid membrane, thereby decreasing both the dynamics of the movement of lipid tails and the average tilt angle of the lipid molecules. The values given in Tables 1 and 2 show that increasing the squalene content from 1% to 1.5% increases bilayer thickness from 5.3 nm to 5.9 nm and the A_n value from 0.049 to 0.062. Futhermore, the increased amount of squalene, by increasing the degree of order of the lipid molecules, also permits a greater packing density and therefore a higher average density of the lipid membrane, which can be seen in Table 2 from the average values of the refractive index (1.503 versus 1.535) and the total mass (7.4 versus 8.7 μmol m^{-2}) for the two membranes. These alterations of the membrane properties have a larger impact, as shown in Fig. 1 *B*, on the second phase of b_6f incorporation than on the first phase. This will be discussed further below.

(2) As Table 2 indicates, despite the increase in the inserted mass of the cyt b_6f complex from 0.007 μmol m^{-2} (or 0.005 μmol m^{-2}) to 0.011 μmol m^{-2} over both phases of incorporation, the total mass of the proteolipid membrane decreases during the second phase from 7.207 μmol m^{-2} (or 8.505 μmol m^{-2}) to 4.011 μmol m^{-2}. This can only be accomplished by removal of lipid.

(3) During the second phase of complex incorporation the molecular order of the lipid-protein layer drastically decreases (A_n values change from 0.048 to 0.026, and from 0.062 to 0.036, for the two membrane systems).

There are some interesting correlations between the changes in mass and molecular order and the membrane characteristics that provide additional information about the structural properties of the system. As the data in Table 2 indicate, the higher the average refractive index of the lipid membrane, n_{av} (i.e., the higher the lipid packing density), the larger the change in the mass of the proteolipid membrane during the second phase (i.e., for both bilayers, the final lipid mass is 4.0 μmol m^{-2}, and the final total mass is 4.011 μmol m^{-2}, despite the differences in the starting values). This correlation also holds for n values obtained

with both *p*- and *s*-polarizations, i.e., because n_p has a higher value than n_s for both lipid membranes, n_p is affected more than n_s by the second phase of cyt b_6f incorporation.

Interaction of plastocyanin with lipid membranes containing cyt b_6f

We have also investigated the interaction between lipid membranes containing the b_6f complex and plastocyanin added to the buffer solution of the CPWR cell at the end of both the first and second phases of cytochrome incorporation. Fig. 4 *A* shows the refractive index of the protein-buffer layer during the first stage of cyt b_6f incorporation into a lipid membrane formed with a solution containing 6 mg/ml egg PC in 1% squalene/butanol (v/v). The solid line represents a hyperbolic fit to the experimental data points and results in an apparent dissociation constant $K_D = 10 \pm 2$ μM and an extrapolated value of the refractive index $n_\infty = 1.41 \pm 0.01$. These two parameters are, within the error limits of the fitting, the same as those of Fig. 3.

Addition of plastocyanin to the solution at the end of this first phase of b_6f incorporation produces two different kinds of resonance changes, depending on the plastocyanin concentration in the CPWR cell. At low plastocyanin concentrations (up to ~25 μM) the resonance position shifts in a manner similar to that of the shift which occurs during the second phase of b_6f complex incorporation (Fig. 1 *B*), i.e., the resonance minimum shifts to smaller incident angles corresponding to a refractive index decrease (shown in Fig. 4 *B*). A hyperbolic fit to these data (*solid line*) yields a dissociation constant $K_D = 10 \pm 1$ μM. In contrast, at plastocyanin concentrations higher than 25 μM the resonance position (and hence the refractive index) shifts in the opposite direction, i.e., the resonance minimum shifts to higher incident angles, as would be expected from a simple binding of plastocyanin to the membrane surface. To confirm this interpretation, we have measured the binding of plastocyanin to a lipid membrane in the absence of b_6f complex (*closed circles* in Fig. 4 *C*) and have compared the results to those obtained with b_6f complex present in the lipid membrane (*open circles* in Fig. 4 *C*; data shown only for the higher plastocyanin concentrations); the solid and dashed lines represent hyperbolic fits to the experimental data. The dissociation constants obtained from these theoretical fits are the same within the limits of error for both data sets, although the adsorbed plastocyanin mass is significantly smaller when b_6f complex is present. These results, taken together with those presented in Fig. 4 *B*, indicate the following two conclusions. First, in the presence of b_6f, plastocyanin binds to both the cytochrome and the membrane, albeit with rather different dissociation constants (10 μM versus 170 μM) and thus different concentration dependencies. Second, the similar values for the dissociation constants shown in Fig. 4 *C* reveal that the lipid membrane remains intact after incorporation of the cyt b_6f complex. The smaller amount of protein bound to the bilayer containing the cyt b_6f complex is expected because of a smaller available membrane surface when the complex is present.

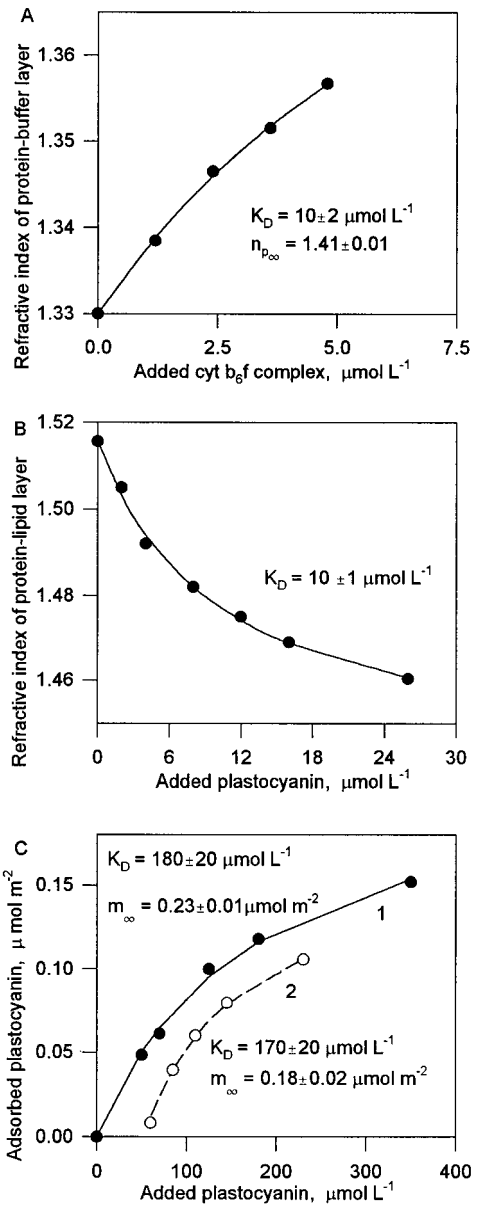

FIGURE 4 Dependence of the refractive index value of either the protein-buffer (*A*) or the protein-lipid (*B*) layer obtained with *p*-polarization and a bilayer membrane containing 6 mg/ml egg PC in butanol/squalene (100:1, v/v) on either the cyt b_6f complex concentration (*A*) or plastocyanin added at the end of the first phase of the b_6f complex incorporation (*B*). (*C*) Plastocyanin binding isotherms to lipid bilayer obtained at high protein concentration, either without (●, ——) or with (○, – – –) cyt b_6f complex after the second phase of protein incorporation. Solid and dashed lines represent nonlinear least-squares fits to a hyperbolic function; these yield the dissociation contants (K_D) and the final value of the refractive index ($n_{p\infty}$) and protein surface coverages (m_∞).

Addition of plastocyanin to the CPWR cell at the end of the second phase of cyt b_6f incorporation results in tighter binding to the complex in the lipid membrane. This is shown in Fig. 5, in which the hyperbolic fit (*solid line*)

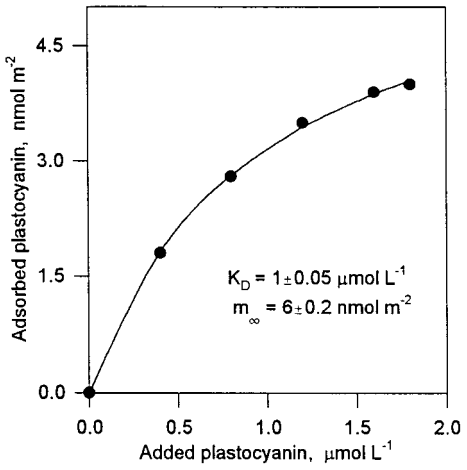

FIGURE 5 Plastocyanin binding isotherm obtained after completion of the second phase of cyt b_6f incorporation. Solid curve shows a nonlinear least-squares fit to a hyperbolic function; this yields the dissociation constant (K_D) and the final protein surface coverage (m_∞).

yields a $K_D = 1 \pm 0.05$ μM, and an extrapolated value of the bound mass at infinite concentration of plastocyanin of 6 ± 0.2 nmol m^{-2}. It is important to note that this dissociation constant value is ~10-fold smaller than that obtained after completion of the first phase of b_6f incorporation (Fig. 4 *B*). We will return to this again below.

The molar ratio of the bound plastocyanin to that of cyt b_6f complex at the end of the second phase can be calculated in two ways. From the hyperbolic fit to the refractive index data in Fig. 3, we can obtain a value for the refractive index of the protein-buffer layer at a concentration of cyt b_6f complex of 8.4 μM in the CPWR cell (i.e., at the end of the second phase of protein incorporation, which corresponds to the maximum amount of b_6f used in these experiments). Applying the Lorentz-Lorenz equation, we are then able to calculate a value for the mass of cyt b_6f incorporated into the lipid membrane (11 nmol m^{-2}; see Table 2). Using this and knowing the mass of bound plastocyanin (6 nmol m^{-2} from Fig. 5), one obtains a ratio of 0.6 ± 0.17. This ratio can also be calculated from the difference between the amount of plastocyanin bound to the bare membrane and that bound to the membrane containing b_6f (Fig. 4 *C*). This mass calculation is based on the fact that curve 2 in Fig. 4 *C* represents the binding of plastocyanin to a smaller lipid membrane surface than in the case of curve 1, because of the b_6f complex that is incorporated at the end of the first phase. Therefore, the difference between the m_∞ values obtained from the two curves in Fig. 4 *C* (50 nmol m^{-2}), mutiplied by the ratio of the surface area occupied by each molecule of plastocyanin (~750 $Å^2$, as calculated from curve 1 in Fig. 4 *C*) to that occupied by a monomeric molecule of cyt b_6f complex (2200 $Å^2$ from the x-ray data; Mosser et al., 1997), yields the mass of the b_6f complex incorporated into the lipid membrane. This gives 17 ± 3.4 nmol m^{-2} of cyt b_6f complex at the end of the second phase of incorporation, and yields a ratio of 0.35 ± 0.07. This value for the mass of b_6f incorporated is larger than that obtained from the refractive index value in Fig. 3 (11 nmol m^{-2}; Table 2).

In the present case, when protein dimensions are larger than the thickness of the lipid bilayer, thereby resulting in a two-layer system (see Fig. 2), both methods of mass calculation have inherent errors. Because of protein dilution in the protein-buffer layer, the first method underestimates the value of the refractive index, which results in a smaller calculated protein mass. The second method assumes that the lipid membrane interacts with water-soluble proteins in the same manner, regardless of the presence or absence of integral membrane protein molecules. Although this seems to be supported by the very similar dissociation constant values obtained under the two conditions (see Fig. 4 *C*), there is still the additional assumption that the entire lipid membrane surface that is not occupied by the integral membrane protein is available to bind a water-soluble protein. That constraint is difficult to verify experimentally, and therefore it may introduce some error, thereby increasing the calculated protein mass. If we average the values obtained with both methods of calculation, one obtains a mass density for the cyt b_6f complex of 14 ± 3.5 nmol m^{-2}. We conclude from this calculation and the extrapolated mass of plastocyanin bound to cyt b_6f complex shown in Fig. 5 (6 ± 0.2 nmol m^{-2}) that one plastocyanin molecule is bound to 2.3 ± 0.6 monomeric cyt b_6f complex molecules at the end of the second phase of incorporation. The simplest interpretation of this result is that two plastocyanin molecues are bound to a dimeric form of those b_6f molecules that are oriented with their plastocyanin-binding sites facing the aqueous phase of the CPWR cell (~50%, assuming random insertion). We will return to this point again below.

DISCUSSION

The results presented above clearly indicate that during the second phase of cyt b_6f incorporation into a planar lipid bilayer the protein-lipid layer undergoes major structural changes. These alterations result in a lower mass density (as indicated by a lower value of the average refractive index) and a lower degree of molecular order (as indicated by the smaller value of the anisotropy) than exist in the original lipid membrane. In addition, the transition between the two phases involves cooperativity, as indicated by the sigmoidal shape of the curves in Fig. 1 *B*, and occurs within a rather small range of protein concentration. Three possible mechanisms can be suggested to account for these results: 1) a protein-induced phase transition within the lipid bilayer; 2) a bimodal association of cyt b_6f with the bilayer; 3) cyt b_6f aggregation within the bilayer. We will discuss these in turn.

It is well known that lipid bilayers in the lamellar phase can undergo transitions that involve major in-plane structural reorganizations (Kinnunen and Laggner, 1991; Israelachvili et al., 1980; Hui and Sen, 1989; Tate et al.,

1991). Decreasing the effective size of the polar headgroup or increasing the effective size of the hydrocarbon chain region will increase the spontaneous curvature of the membrane; if this exceeds a critical energy barrier, it results in the transformation into a nonlamellar phase. In the context of lipid-protein interactions, the degree of mismatch between the thickness of the hydrophobic region of the bilayer and the length of the hydrophobic membrane-spanning domains of an integral protein (Mouritsen and Kinnunen, 1996) is thought to be an essential part of the energetics involved in protein induction of a lamellar to nonlamellar structural transition. The hydrophobic length of the inserted protein enforces a boundary condition on the lipid molecules, which have to adapt their conformational state as well as their local composition to this boundary.

Although hydrophobic matching offers a possible explanation for the structural changes observed during the second phase of cyt b_6f incorporation, there are some experimental data that are somewhat difficult to interpret in this context. For example, the structural changes can also be induced by peripherally bound plastocyanin added at the end of the first phase of b_6f incorporation. Furthermore, the binding affinity of plastocyanin is markedly increased after the structural changes have occurred.

The second possibility involves two modes of b_6f complex association with the lipid bilayer. This mechanism presumes that during the first phase only peripheral binding of the dimer to the membrane occurs. The second phase then would involve insertion of the dimer into the bilayer membrane. The process of incorporation of such a large dimeric complex can reorganize the bilayer in two ways: protein insertion will result in lipid dilution (i.e., lowering the lipid mass and therefore decreasing lipid molecule packing density). Furthermore, the structural arrangement of lipid molecules (due to dilution of the lipid and to protein-lipid interactions) can change. Although these two effects can account for the changes in mass density and anisotropy during the second phase of the cyt b_6f complex incorporation presented in Table 2, again there are other observations that cannot easily be accommodated by this model, i.e., the concentration dependence of the cyt b_6f incorporation mode and the influence of plastocyanin binding on this process.

The third explanation involves the enhancement by the two-dimensional space of the membrane of the probability of formation of dimeric or oligomeric protein complexes due to protein-protein interactions (Grasberger et al., 1986). Such lipid-mediated protein aggregation is known to occur (Mouritsen and Kinnunen, 1996), and both the b_6f and bc_1 complexes are known to dimerize. In the case of the bc_1 complex, it has been proposed that the equilibrium between monomer and dimer plays a role in regulating electron transport in vivo, with the dimeric form having the greater (by a factor of 2–3) activity (Nugent and Bendall, 1987; Nalecz and Azzi, 1985; Schmitt and Trumpower, 1990). Whether or not the b_6f complex is a functional or a structural dimer is still a matter of discussion (Cramer et al., 1994a, 1996; Hope, 1993; Breyton et al., 1997). Radiation inactivation (Nugent and Bendall, 1987) and titration with specific inhibitors (Rich et al., 1991) have indicated that the functional unit is the monomer. On the other hand, although an active monomeric form of the spinach complex has recently been reported (Chain and Malkin, 1995), in most cases the monomeric form of the b_6f complex from higher plants has been found to be much less active (four- to fivefold, or even completely inactive) than the dimeric form (Chain, 1985; Huang et al., 1994). However, even with purification methods that lead to isolation of cyt b_6f complex in a predominantly dimeric form, it has been shown that the conversion of dimer to monomer occurs with time, with a rate dependent on ionic strength. The stability of the dimeric cyt b_6f complex is increased at higher ionic strength (Huang et al., 1994), as has also been found for the cyt bc_1 complex (Nalecz and Azzi, 1985). There also seems to be at least a qualitative similarity between these two complexes as far as the role of lipid is concerned. In both cases lipid molecules stabilize the dimeric form of the complex. Lipid analysis has shown that ~20–30 lipid molecules are present per dimer of the cyt b_6f complex (Breyton et al., 1997; Huang et al., 1994), as compared with the 40–50 molecules of PC per cytochrome c_1 required for maximum activity of the bc_1 complex. Furthermore, as Breyton et al. (1997) have shown with the cyt b_6f complex obtained from *Chlamydomonas reinhardtii*, there seems to be no specificity for lipid molecules for stabilization of the dimer. In addition, they have shown that when the purified b_6f complex was layered onto a gradient containing 20 mM 6-*O*-(*N*-heptylcarbamoyl)-methyl-α-D-glycopyranoside and 0.1 g/liter PC, it sedimented as a mixture of dimeric and monomeric forms, whereas in the presence of 0.2 mM dodecyl-6-D-maltoside and no lipids, the b_6f complex always remained in the dimeric form (Breyton et al., 1997). These latter observations seem to indicate that the presence of lipids shifts the dimer-monomer equlibrium.

Considering the above information and the fact that the purification of the b_6f complex employed in this work yields the dimeric form of the protein, it is possible that dilution of the complex into a lipid membrane results in dimer dissociation and monomer incorporation into the bilayer structure. Such incorporation would occur until the packing density of the inserted protein molecules reaches a high enough level to allow sufficient interaction between protein molecules to lead to the formation of the dimeric state of the cyt b_6f complex. It is possible that the two phases of cyt b_6f incorporation into the lipid membrane observed herein are a consequence of these molecular processes, and that the spectral changes occurring in the second phase arise as a consequence of protein dimerization (note that it is also possible to formulate this mechanism in terms of a dimer-to-oligomer aggregation process, rather than a monomer-to-dimer transition; inasmuch as we have no direct evidence to favor either of these alternatives, we will continue the discussion using the simpler monomer/dimer model). This interpretation is supported by the fact that the second phase of incorporation is governed by a sigmoidal

curve (Fig. 1 *B, curves 2 and 3*), suggesting that cooperativity is involved in this process; such nonlinearity can be associated with dimerization of the complex. Even stronger experimental evidence for dimer formation during the second phase of protein incorporation comes from the experiments on binding of plastocyanin to a membrane containing the b_6f complex, i.e., the induction of structural changes by plastocyanin and the increase in binding affinity after the structural changes have occurred. These results can be simply interpreted as reflecting a tighter binding of plastocyanin to the dimeric form of the protein within the membrane, which acts to shift the equilibrium from monomer to dimer. This explanation is also consistent with the ratio of bound plastocyanin to cyt b_6f incorporated into the lipid membrane (two plastocyanins per dimer), as calculated above.

A dimerization process occurring after protein insertion can result, in general, in larger changes in both mass and proteolipid membrane structure than simple insertion, and can therefore account for the observed decreases in both the average lipid-protein layer packing density and the molecular order of the lipid-protein layer. This is a consequence of monomer reorientation, as well as monomer-monomer interactions resulting in a decrease in the average distance between protein molecules. Furthermore, as recently shown by electron microscopy, the process of b_6f dimerization involves a sequestration of lipid molecules within the dimer interface (Breyton et al., 1997). Such a boundary phase of lipid molecules would be expected to have a molecular orientation rather different from that of the bulk lipid phase, thereby contributing to the observed changes in the order parameter. It is also possible that protein aggregation could favor localized lamellar-to-nonlamellar phase transitions.

Although the monomer/dimer model accounts for all of the experimental results presented in this work, there is no direct evidence in the literature that the monomer-to-dimer association can be reversibly accomplished. Furthermore, removal of Rieske protein has often been observed to accompany the monomerization of the complex. This is consistent with electron microscopy (Mosser et al., 1997) data that suggest the Rieske protein lies close to the monomer/monomer interface, which might explain why its loss and monomerization of the complex generally occur concomitantly. In contrast to this, Breyton et al. (1997) have recently suggested the existence of an intermediate monomeric form of the complex retaining all seven subunits, generated by dilution of the dimer into a large pool of detergent micelles. Furthermore, they argue that the possibility of existence of a monomeric form containing the Rieske protein is substantiated by its transient presence during purification of the small subunit of the cyt b_6f complex (Takahashi et al., 1996).

Based on the above discussion, it is clear that additional work will be required to evaluate the monomer/dimer model presented herein. Thus it would be of interest to vary the lipid composition in the bilayer so as to favor the occurrence of phase transitions (e.g., by including phosphatidylethanolamine), as well as to represent a more physiological situation (e.g., by including galactolipids). It will be especially important to examine the electron transport activity of the cyt b_6f complex over both phases of protein incorporation within a supported lipid bilayer, which can be accomplished by simultaneously measuring CPWR spectra and electrochemical redox processes. Such studies are under way.

Supported in part by National Science Foundation grant MCB-9404702 (to ZS and GT) and National Institutes of Health grant GM-38323 (to WAC).

REFERENCES

Bald, D., J. Kruip, E. J. Boekema, and M. Rögner. 1992. Structural investigations on cytB6/f-complex and PSI-complex from the cyanobacterium *Synechocystis* PCC6803. *In* Research in Photosynthesis, Vol. 1. N. Murata, editor. Kluwer, Dordrecht. 629–632.

Boekema, E. J., A. F. Boonstra, J. P. Dekker, and M Rögner. 1994. Electron microscopic structural analysis of photosystem I, photosystem II, and the cytochrome b_6f complex from green plants and cyanobacteria. *J. Bioenerg. Biomembr.* 26:17–24.

Breyton, C., C. de Vitry, and J. L. Popot. 1994. Membrane association of cytochrome b_6f subunits. *J. Biol. Chem.* 269:7597–7602.

Breyton, C., Ch. Tribet, J. Olive, J.-P. Dubacq, and J.-L. Popot. 1997. Dimer to monomer conversion of the cytochrome b_6f complex. *J. Biol. Chem.* 272:21892–21900.

Brown, M. F. 1994. Modulation of rhodopsin function by properties of the membrane bilayer. *Chem. Phys. Lipids.* 73:159–180.

Chain, R. K. 1985. Involvement of plastoquinone and lipids in electron transport reactions mediated by the cytochrome b_6f complex isolated from spinach. *FEBS Lett.* 180:321–325.

Chain, R. K., and R. Malkin. 1995. Functional activities of monomeric and dimeric forms of the chloroplast cytochrome b_6f complex. *Photosynth. Res.* 46:419–426.

Cramer, W. A., P. N. Furbacher, A. Szczepaniak, and G. S. Tae. 1991. Electron transport between photosystem II and photosystem I. *In* Current Topics in Bioenergetics. C. P. Lee, editor. Academic Press, San Diego. 179–222.

Cramer, W. A., S. E. Martinez, P. N. Furbacher, D. Huang, and J. L. Smith. 1994a. The cytochrome b_6f complex. *Curr. Opin. Struct. Biol.* 4:536–544.

Cramer, W. A., S. E. Martinez, D. Huang, G.-S. Tae, R. M. Everly, J. B. Heymann, R. H. Cheng, T. S. Baker, and J. L. Smith. 1994b. Structural aspects of the cytochrome b_6f complex: structure of the lumen-side domain of cytochrome f. *J. Bioenerg. Biomembr.* 26:31–47.

Cramer, W. A., G. M. Soriano, M. Ponomarev, D. Huang, H. Zhang, S. E. Martinez, and J. L. Smith. 1996. Some new structural aspects and old controversies concerning the cytochrome b_6f complex of oxygenic photosynthesis. *Annu. Rev. Plant Physiol. Plant Mol. Biol.* 47:477–508.

Culis, P. R., and B. De Kruijf. 1979. Lipid polymorphism and the functional roles of lipids in biological membranes. *Biochim. Biophys. Acta.* 559:399–420.

Den Engelsen, D. 1976. Optical anisotropy in ordered systems of lipids. *Surf. Sci.* 56:272–280.

Epand, R. M. 1991. Relationship of phospholipid hexagonal phases to biological phenomena. *Chem.-Biol. Interact.* 63:239–247.

Gee, M. L., T. W. Healy, and L. R. White. 1990. Hydrophobicity effects in the condensation of water films on quartz. *J. Colloid Interface Sci.* 140:450–465.

Grasberger, B., A. P. Minton, C. DeLisi, and H. Metzger. 1986. Interaction between proteins localized in membranes. *Proc. Natl. Acad. Sci. USA.* 83:6258–6262.

Gross, E. L. 1993. Plastocyanin: structure and function. *Photosynth. Res.* 34:359–374.

Guss, J. M., H. D. Bartunik, and H. C. Freeman. 1992. Accuracy and precision in protein crystal structure analysis: restrained least-squares refinement of the crystal structure of poplar plastocyanin at 1.33 angstroms resolution. *Acta Crystallogr. B.* 48:790–811.

Heimburg, T., and D. Marsh. 1996. Thermodynamics of the interaction of proteins with lipid membranes. *In* Biological Membranes. K. Merz, Jr., and B. Roux, editors. Birkhäuser, Boston. 405–462.

Hope, A. B. 1993. The chloroplast cytochrome bf complex: a critical focus on function. *Biochim. Biophys. Acta.* 1143:1–22.

Huang, D., R. M. Everly, R. H. Cheng, J. B. Heymann, H. Schägger, V. Sled, T. Ohnishi, T. S. Baker, and W. A. Cramer. 1994. Characterization of the chloroplast cytochrome b_6f complex as a structural and functional dimer. *Biochemistry.* 33:4401–4409.

Hui, S. W., and A. Sen. 1989. Effects of lipid packing on polymorphic phase behaviour and membrane properties. *Proc. Natl. Acad. Sci. USA.* 86:5825–5829.

Israelachvili, J. N., S. Marcelja, and R. G. Horn. 1980. Physical principles of membrane organization. *Q. Rev. Biophys.* 13:121–200.

Jordi, W., and B. de Kruijff. 1995. Apo- and holocytochrome *c*-membrane interactions. *In* Cytochrome *c*: A Multidisciplinary Approach. R. A. Scott and A. G. Mauk, editors. University Science Books, Sausalito, CA. 449–474.

Kinnunen, P. K. J., and P. Laggner. 1991. Phospholipid phase transitions. *Chem. Phys. Lipids.* 57:109–408.

Martinez, S. E., D. Huang, A. Szczepaniak, W. A. Cramer, and J. L. Smith. 1994. Crystal structure of chloroplast cytochrome *f* reveals a novel cytochrome fold and unexpected heme ligation. *Structure.* 2:95–105.

Meyer, T. E., Z. G. Zhao, M. A. Cusanovich, and G. Tollin. 1993. Transient kinetics of electron transfer from a variety of *c*-type cytochromes to plastocyanin. *Biochemistry.* 32:4552–4559.

Mosser, G., C. Breyton, A. Olofsson, J.-L. Popot, and J.-L. Rigaud. 1997. Projection map of cytochrome b_6f complex at 8 Å resolution. *J. Biol. Chem.* 272:20263–20268.

Mouritsen, O. G., and K. J. Kinnunen. 1996. Role of lipid organization and dynamics for membrane functionality. *In* Biological Membranes. K. Merz, Jr., and B. Roux, editors. Birkhäuser, Boston. 463–502.

Mueller, P., D. O. Rudin, H. T. Tien, and W. C. Wescott. 1962. Reconstitution of cell membrane structure in vitro and its transformation into an excitable system. *Nature.* 194:979–980.

Nalecz, M. J., and A. Azzi. 1985. Functional characterization of the mitochondrial cytochrome bc_1 complex: steady-state kinetics of the monomeric and dimeric forms. *Arch. Biochem. Biophys.* 240:921–931.

Nugent, J. H. A., and D. S. Bendall. 1987. Functional size measurements on the chloroplast cytochrome b_6f complex. *Biochim. Biophys. Acta.* 893:177–183.

Pearson, D. L., E. L. Gross, and E. S. David. 1996. Electrostatic properties of cytochrome *f*: implications for docking with plastocyanin. *Biophys. J.* 71:64–76.

Pelzl, G. 1994. Thermodynamic behavior and physical properties of thermotropic liquid crystals. *In* Topics in Physical Chemistry, Vol. 3, Liquid Crystals. H. Stegemeyer, editor. Steinkopf, Springer Verlag, Berlin.

Pinheiro, T. J. T., G. A. Elöve, A. Watts, and H. Roder. 1997. Structural and kinetic description of cytochrome *c* unfolding induced by the interaction with lipid vesicles. *Biochemistry.* 36:13122–13132.

Qin, L., and N. M. Kostic. 1993. Importance of protein rearrangement in the electron-transfer reaction between the physiological partners cytochrome *f* and plastocyanin. *Biochemistry.* 32:6073–6080.

Rich, P. R., S. A. Madwick, and D. A. Moss. 1991. The interactions of duraquinol, DBMIB and NQNO with chloroplast cytochrome *bf* complex. *Biochim. Biophys. Acta.* 1058:312–327.

Salamon, Z., H. A. Macleod, and G. Tollin. 1997a. Coupled plasmon-waveguide resonators: a new spectroscopic tool for probing proteolipid film structure and properties. *Biophys. J.* 73:2791–2797.

Salamon, Z., H. A. Macleod, and G. Tollin. 1997b. Surface plasmon resonance spectroscopy as a tool for investigating the biochemical and biophysical properties of membrane protein systems. I. Theoretical principles. *Biochim. Biophys. Acta.* 1331:117–129.

Salamon, Z., H. A. Macleod, and G. Tollin. 1997c. Surface plasmon resonance spectroscopy as a tool for investigationg the biochemical and biophysical properties of membrane protein systems. II. Applications to biological systems. *Biochim. Biophys. Acta.* 1331:131–152.

Salamon, Z., and G. Tollin. 1992. Direct electrochemistry of spinach plastocyanin at a lipid bilayer-modified electrode: cyclic voltammetry as a probe of membrane-protein interactions. *Arch. Biochem. Biophys.* 294:382–387.

Salamon, Z., and G. Tollin. 1996a. Surface plasmon resonance studies of complex formation between cytochrome *c* and bovine cytochrome *c* oxidase incorporated into a supported planar lipid bilayer. I. Binding of cytochrome *c* to cardiolipin/phosphatidylcholine membranes in absence of oxidase. *Biophys. J.* 71:848–857.

Salamon, Z., and G. Tollin. 1996b. Surface plasmon resonance studies of complex formation between cytochrome *c* and bovine cytochrome *c* oxidase incorporated into a supported planar lipid bilayer. II. Binding of cytochrome *c* to oxidase-containing cardiolipin/phosphatidylcholine membranes. *Biophys. J.* 71:858–867.

Salamon, Z., and G. Tollin. 1997. Interaction of horse heart cytochrome *c* with lipid bilayer membranes: effects on redox potentials. *J. Bioenerg. Biomembr.* 29:211–221.

Salamon, Z., and G. Tollin. 1998. Surface plasmon resonance spectroscopy: a new biophysical tool for probing membrane structure and function. *In* Biomembrane Structure. D. Chapman and P. Haris, editors. IOS Press, Amsterdam. 186–204.

Salamon, Z., Y. Wang, M. F. Brown, H. A. Macleod, and G. Tollin. 1994. Conformational changes in rhodopsin probed by surface plasmon resonance spectroscopy. *Biochemistry.* 33:13706–13711.

Salamon, Z., Y. Wang, J. L. Soulages, M. F. Brown, and G. Tollin. 1996. Surface plasmon resonance spectroscopy studies of membrane proteins: transducin binding and activation by rhodopsin monitored in thin membrane films. *Biophys. J.* 71:283–294.

Schmitt, M. E., and B. L. Trumpower. 1990. Subunit 6 regulates half-of-the-site reactivity of the dimeric cytochrome bc_1 complex in *Saccharomyces cerevisiae. J. Biol. Chem.* 265:17005–17011.

Sigfridsson, K., S. Young, and Ö. Hansson. 1997. Electron transfer between spinach plastocyanin mutants and photosystem I. *Eur. J. Biochem.* 245:805–812.

Silberzan, P., L. Leger, D. Ausserre, and J. J. Benattar. 1991. Silanation of silica surfaces. A new method of constructing pure or mixed monolayers. *Langmuir.* 7:1647–1651.

Singer, S. J., and G. L. Nicolson. 1972. The fluid mosaic model of the structure of cell membranes. *Science.* 173:720–731.

Soriano, G. M., M. V. Ponamarev, G.-S. Tae, and W. A. Cramer. 1996. Effect of the interdomain basic region of cytochrome *f* on its redox reactions in vivo. *Biochemistry.* 35:14590–14598.

Szczepaniak, A., D. Huang, T. W. Keenan, and W. A. Cramer. 1991. Electrostatic destabilization of the cytochrome b_6f complex in the thylakoid membrane. *EMBO J.* 10:2757–2764.

Takahashi, Y., M. Rahire, C. Breyton, J.-I. Popot, P. Joliot, and J.-D. Rochaix. 1996. The chloroplast ycf (pet L) open reading frame of *Chlamydomonas reinhardtii* encodes a small functionally important subunit of cytochrome b_6f complex. *EMBO J.* 15:3498–3506.

Tate, M. W., E. F. Eikenberry, D. C. Turner, E. Shyamsunder, and S. M. Gruner. 1991. Nonbilayer phases of membrane lipids. *Chem. Phys. Lipids.* 57:147–164.

Thoma, M., M. Schwendler, H. Baltes, C. A. Helm, T. Pfohl, H. Riegler, and H. Möhwald. 1996. Ellipsometry and x-ray reflectivity studies on monolayers of phosphatidylethanolamine and phosphatidylcholine in contact with *n*-dodecane, *n*-hexadecane and bicyclohexyl. *Langmuir.* 12:1722–1728.

Xia, D., Ch.-A. Yu, H. Kim, J.-Z. Xia, A. M. Kachurin, L. Zhang, L. Yu, and J. Deisenhofer. 1997. Crystal structure of the cytochrome bc_1 complex from bovine heart mitochondria. *Science.* 277:60–66.

Yocum, C. F. 1982. Purification of ferredoxin and plastocyanin. *In* Methods in Chloroplast Molecular Biology. M. Edelman, R. B. Hallick, and N. H. Chua, editors. Elsevier Biomedical Press, Amsterdam, the Netherlands. 973–981.